The QCD CEP in the 3 flavoured constituent quark model

Péter Kovács

HAS-ELTE Statistical and Biological Physics Research Group

Rab, aug. 30 - sept. 3, 2007

- Motivation for using effective models to describe the QCD CEP
- The model and its parametrization for zero and non-zero μ_B, μ_I, μ_Y chemical potential
- The location and the scaling region of the CEP at $\mu_I = \mu_Y = 0$
- Introduction of the chemical potentials: μ_B, μ_I, μ_Y
- Effects of isospin breaking on the location of the CEP
- Conclusions

Collaborator: Zs. Szép

Contradicting lattice results, and the role of effective models

The physical point is in the crossover regime. Y. Aoki, *et al.*, Nature 443, 675 (2006)

Envisaged chiral critical surfaces from lattice simulations:

F. Karsch, J.Phys. G31 (2005) S351

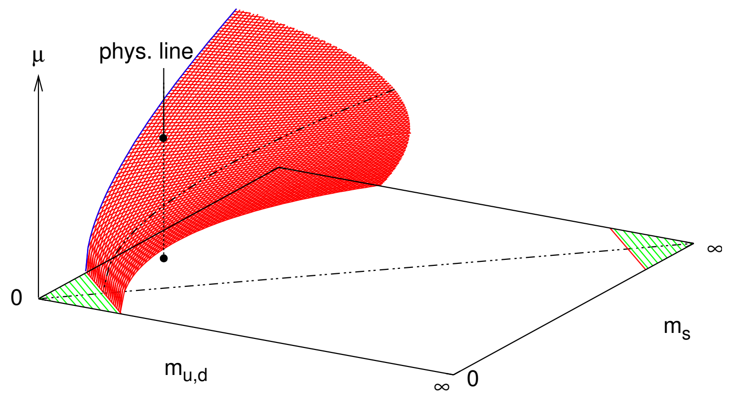

O. Philipsen, Ph. de Forcrand, hep-lat/0607017

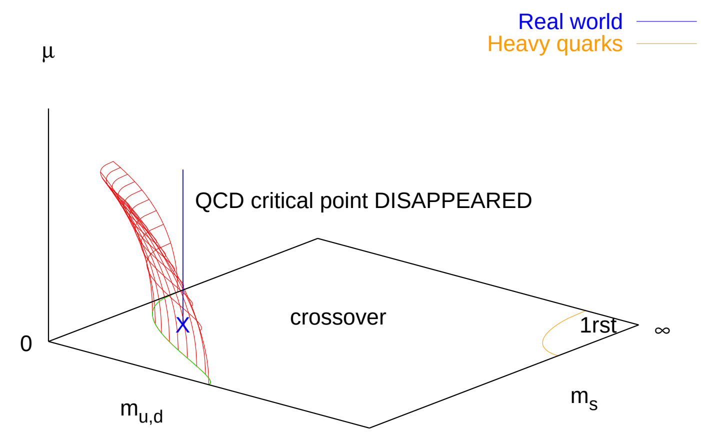

The common expectation is that this surface bends towards the physical point.

However negative curvature according to O. Philipsen, Ph. de Forcrand, hep-lat/0607017

CEP found at:

$T_{\rm CEP} = 160 \pm 3.5$ MeV $\mu_{\rm B,CEP} = 725 \pm 35$ MeV, lattice volume: 12×4^3 and $m_\pi \approx 2 m_\pi^{\rm phys}$ Z. Fodor, S. D. Katz, JHEP 0203:014,2002

$T_{\rm CEP} = 162 \pm 2$ MeV $\mu_{\rm B,CEP} = 360 \pm 40$ MeV, lattice volume: 12×4^3 and $m_\pi = m_\pi^{\rm phys}$ Z. Fodor, S. D. Katz, JHEP 0404:050,2004

The simulation at finite μ is very difficult.

$\longrightarrow$ qualitative difference between lattice results $\longrightarrow$ role of effective models

Relevance of the study of the CEP

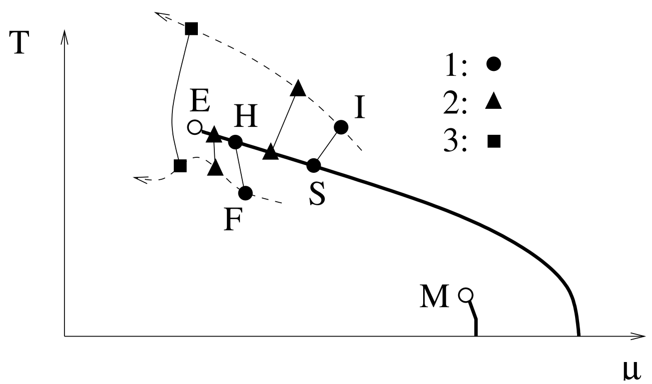

the CEP is experimentally accesible
$\mu_B, \mu_I \neq 0$ in heavy ion collison experiments
μ_B is tunable $\rightarrow$ beam energy, centrality
μ_I is tunable $\rightarrow$ different isotopes of an element
focusing effect: if CEP exist it cannot be missed

analogy to the CEP of a liquid-gas phase transition which is easy to hit

lattice simulation at μ_B is very difficult

$\Longrightarrow$ not all the methods predict/find the CEP

CEP found at: $(T, \mu_B)_{\rm CEP} = (162 \pm 2, 360 \pm 40)$ MeV, volume: 12×4^3 and $m_\pi = m_\pi^{\rm phys}$

Z. Fodor, S. D. Katz, JHEP 0404:050,2004

lattice simulation at μ_I is free of the sign problem

it is important to study the CEP and its μ_I, μ_Y dependence in effective models

Influence of μ_I on the $\mu_B - T$ diagram

Barducci et. al, PLB **564**, 217

without $U(1)_A$ breaking $\rightarrow$ generic result
for low T μ_I induces two 1$^{\text{st}}$ order transitions
$\Longrightarrow$ 2 critical endpoints

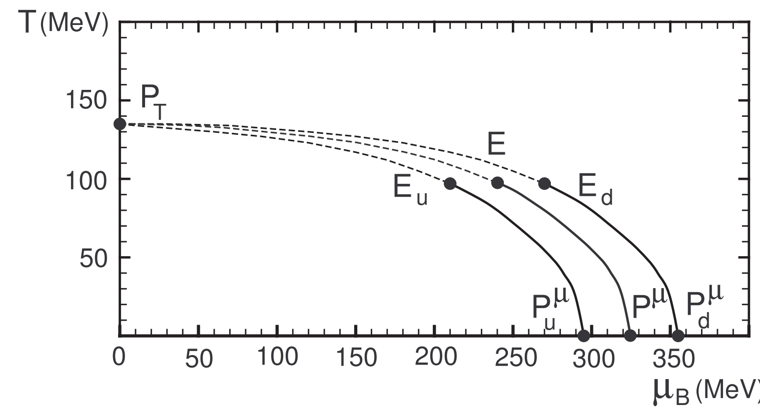

the structure cease to exist in case of a sufficiently strong $U(1)_A$ breaking

Frank et. al, PLB **562**, 221

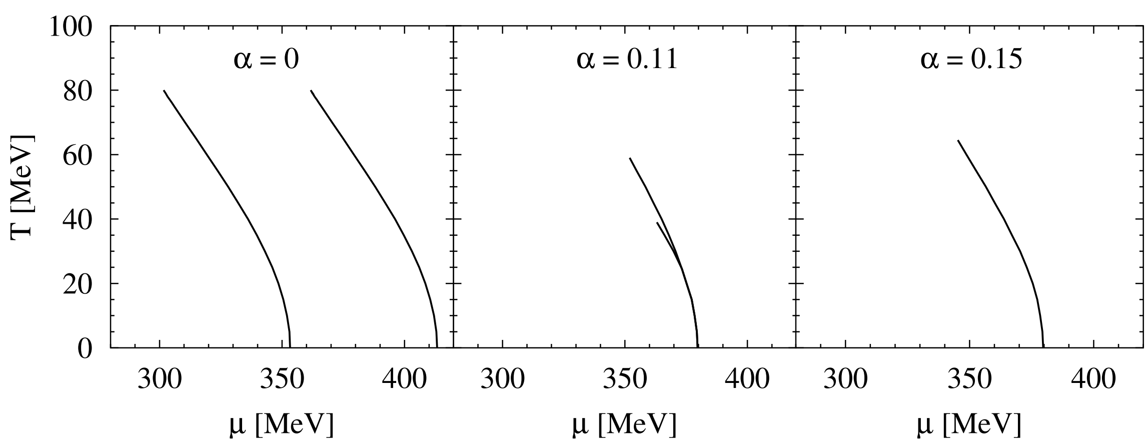

$SU_L(3) \times SU_R(3)$ symmetric chiral quark model

$$\mathcal{L} = \frac{1}{2}\mathrm{Tr}(\partial_\mu M^\dagger \partial^\mu M + m_0^2 M^\dagger M) - f_1 \left(\mathrm{Tr}(M^\dagger M)\right)^2 - f_2 \mathrm{Tr}(M^\dagger M)^2$$
$$- g\left(\det(M) + \det(M^\dagger)\right) + \epsilon_0\sigma_0 + \epsilon_3\sigma_3 + \epsilon_8\sigma_8 + \bar\psi\left(i\partial\!\!\!/ - g_F M_5\right)\psi.$$

$M = \frac{1}{\sqrt{2}}\sum_{i=0}^{8}(\sigma_i + i\pi_i)\lambda_i$, $M_5 = \sum_{i=0}^{8}\frac{1}{2}(\sigma_i + i\gamma_5\pi_i)\lambda_i$ 3×3 complex matrices

pseudo(scalar) fields: π_i, σ_i, quark field: $\bar\psi = (u, d, s)$

Gell-Mann matrices: $\lambda_0 := \sqrt{\frac{2}{3}}\mathbf{1}$, $\lambda_i \;:\; i = 1\ldots 8.$

determinant breaks $U_A(1)$ symmetry
explicit symmetry breaking: external fields $\epsilon_0, \epsilon_3, \epsilon_8 \neq 0 \Longleftrightarrow m_u \neq m_d \neq 0, m_s \neq 0$

broken symmetry phase: three condensates $(\langle\sigma_0\rangle, \langle\sigma_8\rangle), \langle\sigma_3\rangle \longleftrightarrow (x, y), v_3$
x: non-strange, y: strange

fermion masses: $M_u = \frac{g_F}{2}(x + v_3)$, $M_d = \frac{g_F}{2}(x - v_3)$, $M_s = \frac{g_F y}{\sqrt{2}}$

technical difficulty: mixing in the $0, 3, 8$ sector

parameters determined from the $T = 0$ mass spectrum

Parametrization and thermodynamics at one-loop level

13 unknown parameters:

couplings	m_0^2, f_1, f_2, g, g_F
condensates	x, y, v_3
external fields	$\epsilon_x, \epsilon_y, \epsilon_3$
renormalization scales	l_f, l_b

resummation using optimized perturbation theory   Chiku & Hatsuda, PRD58:076001

change: $-m_0^2 \to m^2 \quad \Rightarrow \quad \mathcal{L}_{mass} = \frac{1}{2}m^2 \mathrm{Tr} M^\dagger M - \frac{1}{2}\underbrace{(m_0^2 + m^2)}_{\Delta m^2:\text{ one-loop counterterm}} \mathrm{Tr} M^\dagger M$

principle of minimal sensitivity $\quad M_\pi^2 = iG^{-1}(p^2=0)\big|_{\text{1-loop}} \stackrel{!}{=} m_\pi^2\big|_{\text{tree}} \Longrightarrow$ equation for the effective mass:

$$m^2 = -m_0^2 + \Sigma_\pi(p=0, m_i(m^2), M_q)$$

From the tree-level pion mass: $m^2 = m_\pi^2 - (4f_1 + 2f_2)x^2 - 4f_1 y^2 - 2gy$

$\Longrightarrow$ introducing into the other tree-level masses

$\Longrightarrow$ self-consistent gap equation for the pion mass

Set of coupled nonlinear equations (for $v_3 = 0$):

(1) gap-equation: $$m_\pi^2 = -m_0^2 + (4f_1 + 2f_2)x^2 + 4f_1 y^2 + 2gy + \mathrm{Re}\Sigma_\pi(p=0, m_i(m_\pi), M_u)$$

(2) pole-mass M_K from:

$$M_K^2 = -m_0^2 + 2(2f_1 + f_2)(x^2 + y^2) + 2f_2 y^2 - \sqrt{2}x(2f_2 y - g) + \mathrm{Re}\Sigma_K(p^2 = M_K^2, m_i)$$

(3) FAC criterion for M_K: $$\Sigma(p^2 = M_K^2) = 0$$

(4) pole-mass M_η from:

$$\mathrm{Det}\begin{pmatrix} p^2 - m_{\eta xx}^2 - \Sigma_{\eta xx}(p^2, m_i) & -m_{\eta xy}^2 - \Sigma_{\eta xy}(p^2, m_i) \\ -m_{\eta xy}^2 - \Sigma_{\eta xy}(p^2, m_i) & p^2 - m_{\eta yy}^2 - \Sigma_{\eta yy}(p^2, m_i) \end{pmatrix}\Bigg|_{p^2 = M_\eta^2, M_{\eta'}} = 0$$

(5) PCAC: $$x = f_\pi$$

(6) From non-strange quark mass: $$g_F = \frac{2M_u}{x}$$

(7) From strange quark mass: $$y = \frac{\sqrt{2}M_s}{g_\mathrm{F}}$$

(8) EOS for x:

$$\epsilon_x = -m_0^2 x + 2gxy + 4f_1 xy^2 + 2(2f_1 + f_2)x^3 + \sum_{\alpha,i,j} t^x_{\alpha_{i,j}} \langle \alpha_i \alpha_j \rangle + \frac{g_F}{2}(\langle \bar{u}u \rangle + \langle \bar{d}d \rangle)$$

(9) EOS for y: $$\epsilon_y = -m_0^2 y + gx^2 + 4f_1 x^2 y + 4(f_1 + f_2)y^3 + \sum_{\alpha,i,j} t^y_{\alpha_{i,j}} \langle \alpha_i \alpha_j \rangle + \frac{g_F}{\sqrt{2}} \langle \bar{s}s \rangle$$

Differences in case of isospin breaking

New variable: v_3
Equation for $v_3 \longrightarrow$ third EoS:

$$\langle \frac{\partial \mathcal{L}}{\partial \sigma_3} \rangle = 0 \qquad (1)$$

Even if $\epsilon_3 = 0$ ($\Longrightarrow v_3 = 0$ at $T = 0$) non zero μ_I will generate v_3 at non zero temperature

Cosequence: charged and neutral particle masses will be different at tree level

If explicit isospin breaking is also introduced another equation is needed:

$$m_{\pi^+,\text{tree}} - m_{\pi^0,\text{tree}} = 4.594 MeV \qquad (2)$$

This equation will determine v_3 at $T = 0$ and EoS for v_3 at $T = 0$ will determine ϵ_3

Deviation from the physical mass spectrum

The remaining two unknown parameters, l_f and l_b are determined trough accurate parametrization

Better parametrization $\longleftrightarrow$ closer to the physical spectrum

$$R = \frac{1}{|T|}\sum_{i\in T}\frac{|m_i^{\text{tree}} - m_i^{\text{phys}}|}{m_i^{\text{phys}}} + \frac{1}{|L|}\sum_{i\in L}\frac{|m_i^{\text{tree}} - m_i^{\text{1-loop}}|}{m_i^{\text{tree}}},$$

$$T = \{\eta, \eta', a_0, f_0, \sigma\},\ L = \{\eta', a_0, \kappa, f_0\}, |T| = 5,\ |L| = 4.$$

Physical mass spectrum:

$$\begin{array}{ll} m_\pi = 138 \text{ MeV} & m_{a_0} = 980 \text{ MeV} \\ m_K = 495.6 \text{ MeV} & m_\kappa = 900 \text{ MeV} \\ m_\eta = 547.8 \text{ MeV} & m_{f_0} = 1370 \text{ MeV} \\ m_{\eta'} = 958 \text{ MeV} & m_\sigma = 700 \text{ MeV} \end{array}$$

The closer we are to the physical spectrum the smaller R we get.

$\Longrightarrow$ We have located the minimum of R.

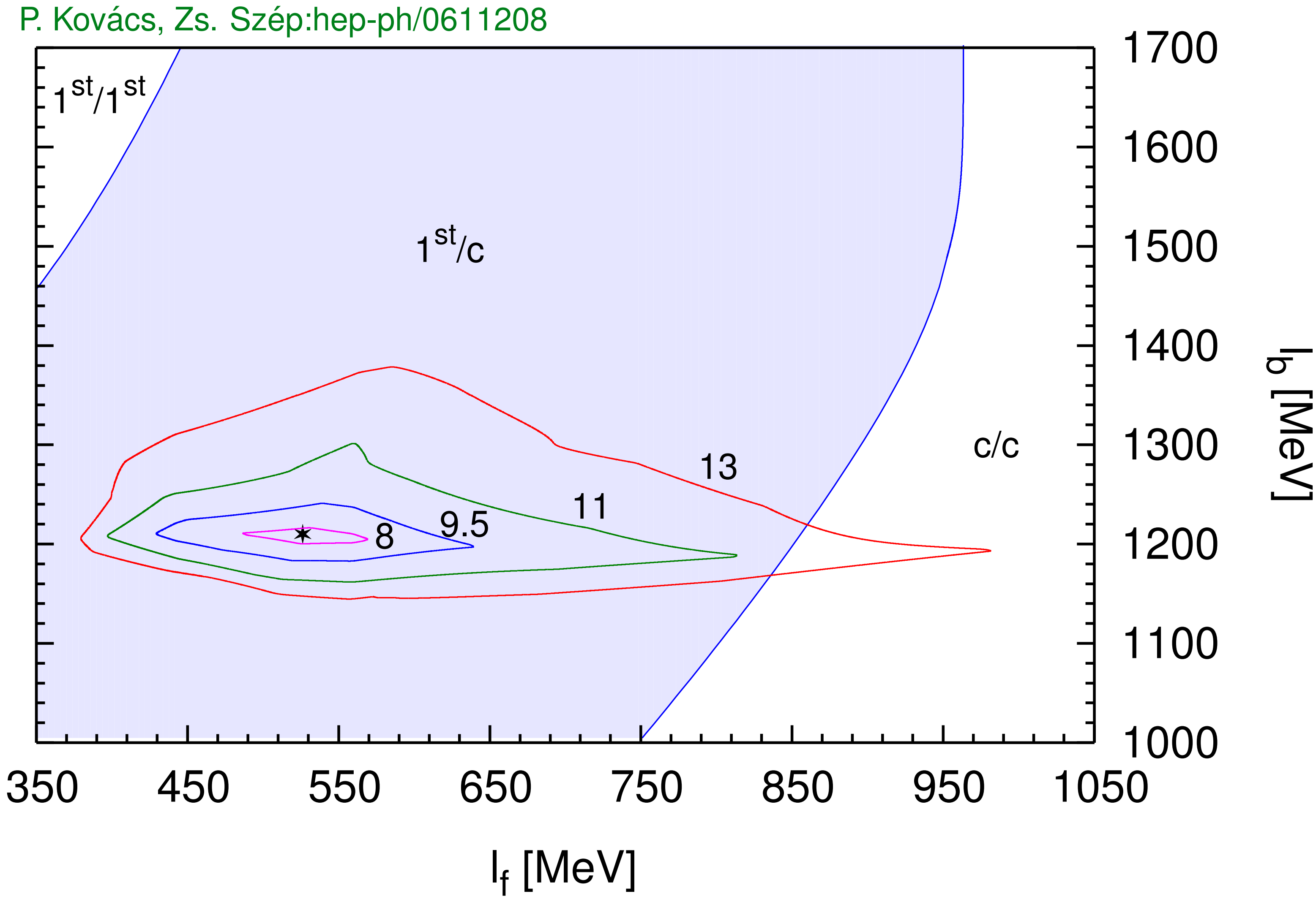

Star on fig.: $l_b = 520$ MeV, $l_f = 1210$ MeV $\longrightarrow$ corresponds to the minimum of R

1-loop masses of σ and f_0: $m_\sigma = 614.2$ MeV, $m_{f_0} = 1210.9$ MeV

Close to the physical spectrum, the phase transition is of first order / crossover type on the $T = 0$ / $\mu_B = 0$ axes.

The surface of 2^{nd} order phase transition in the $m_{u,d} - m_s - \mu_B$ space

Away from the physical point we re-parametrized the model using CHPT

$\longrightarrow$ for mesons in the large N_c limit for f_π, m_η: P. Herrera-Siklódy *et al.*, PLB 419 (1998) 326

$$f_\pi = f\left(1 + 4L_5\frac{m_\pi^2}{f^2}\right)$$

$$m_\eta^2 = \frac{4m_K^2 - m_\pi^2}{3} + \frac{32}{3}(2L_8 - L_5)\frac{\left(m_K^2 - m_\pi^2\right)^2}{f^2},$$

$\longrightarrow$ for baryons ($B \in \{N, \Sigma, \Lambda, \Xi, \}$): V. Bernard *et al.*, Int. J. Mod. Phys. **E4**, 193 (1995)

$$M_B = M_0 - 2b_0(m_{\pi,2}^2 + m_{K,2}^2) + b_D\gamma_B^D(m_\pi, m_K) + b_F\gamma_B^F(m_\pi, m_K) - \frac{1}{24\pi f^2}\left[\alpha_B^\pi m_\pi^3 + \alpha_B^K m_K^3 + \alpha_B^\eta m_\eta^3\right]$$

The constituent kvark masses:

$$m_u = \frac{M_N(m_\pi, m_K)}{3}$$

$$m_s = \frac{M_\Lambda(m_\pi, m_K) + M_\Sigma(m_\pi, m_K)}{2} - 2M_u(m_\pi, m_K)$$

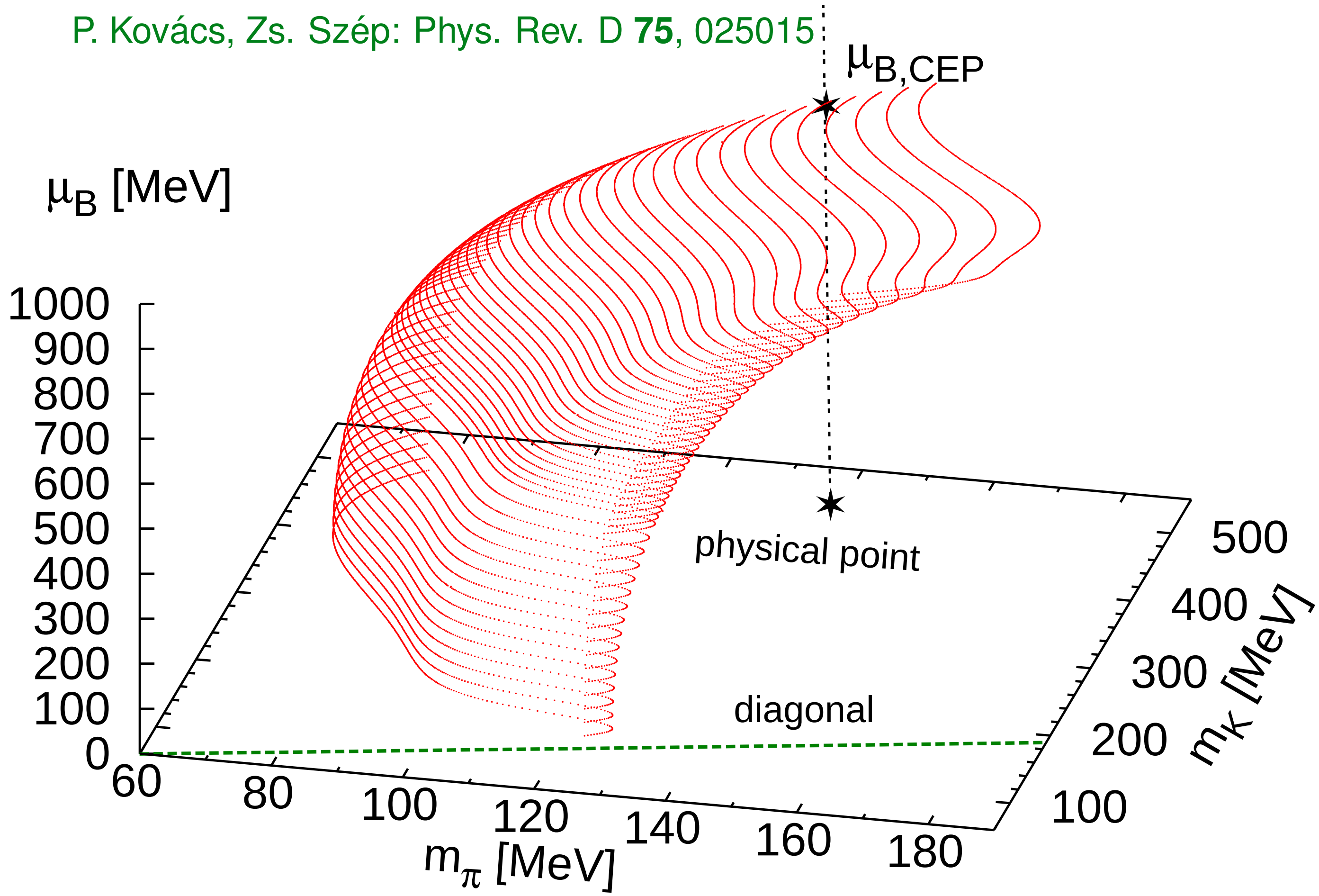

The surface bends towards the physical point $\Longrightarrow$ The CEP must exist

The continuation is reliable up to $m_K \approx 400$ MeV and above the diagonal

The CEP at the physical point of the mass plane

P. Kovács, Zs. Szép: Phys. Rev. D **75**, 025015

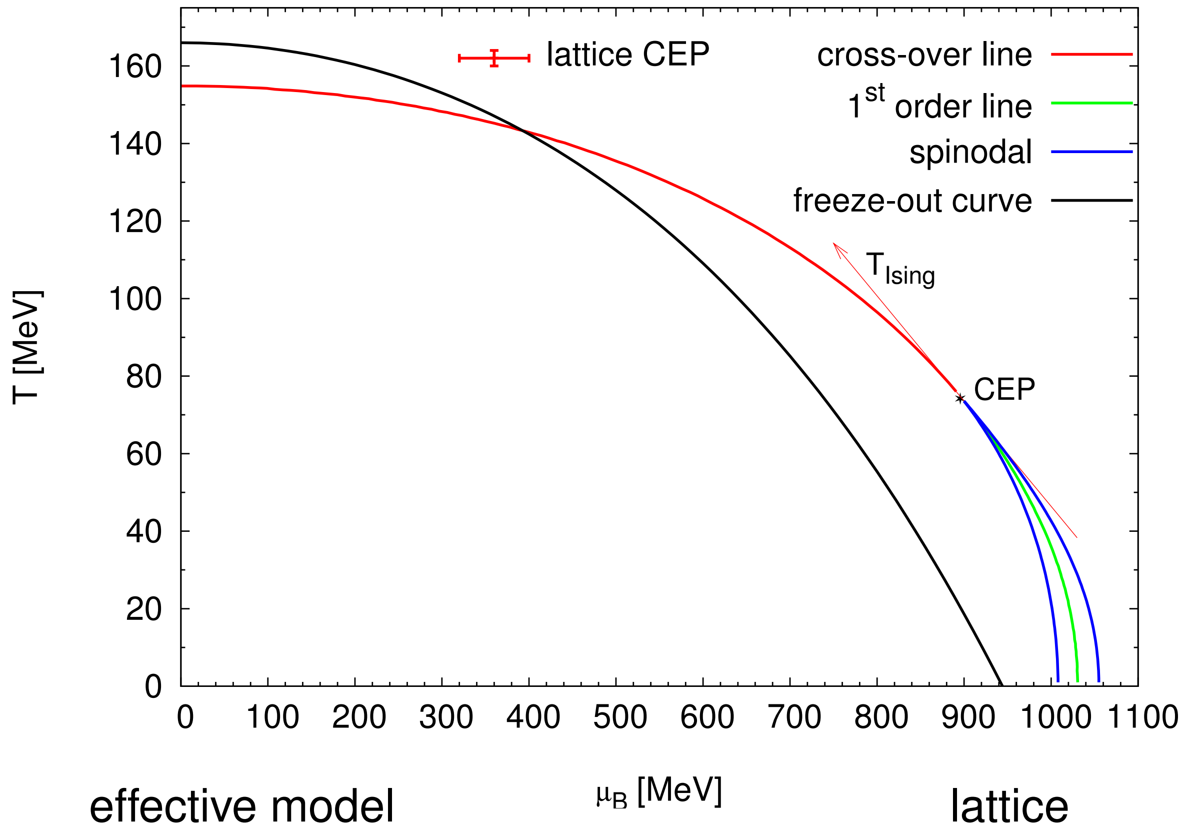

effective model	lattice
• $T_c(\mu_B = 0) = 154.84$ MeV $\Delta T_c(x\chi) = 15.5$ MeV	• $T_c(\mu_B = 0) = 151(3)$ MeV $\Delta T_c(\chi_{\bar{\psi}\psi}) = 28(5)$ MeV Y. Aoki, *et al.*, PLB **643**, 46 (2006)
• $T_{CEP} = 74.83$ MeV $\mu_{B,CEP} = 895.38$ MeV	• $T_{CEP} = 162(2)$ MeV $\mu_{B,CEP} = 360(40)$ MeV
• $T_c \frac{d^2 T_c}{d\mu_B^2}\Big\|_{\mu_B=0} = -0.09$	• $-0.058(2)$ Z. Fodor, *et al.*, JHEP 0404 (2004) 050

Dependence of the $\mu_{B,CEP}$ on the width of the susceptibility

$\mu_{\mathrm{B,CEP}} = 725(35)$ MeV $\longrightarrow$ non-physical quark mass

$\mu_{\mathrm{B,CEP}} = 360(40)$ MeV $\longrightarrow$ physical quark mass

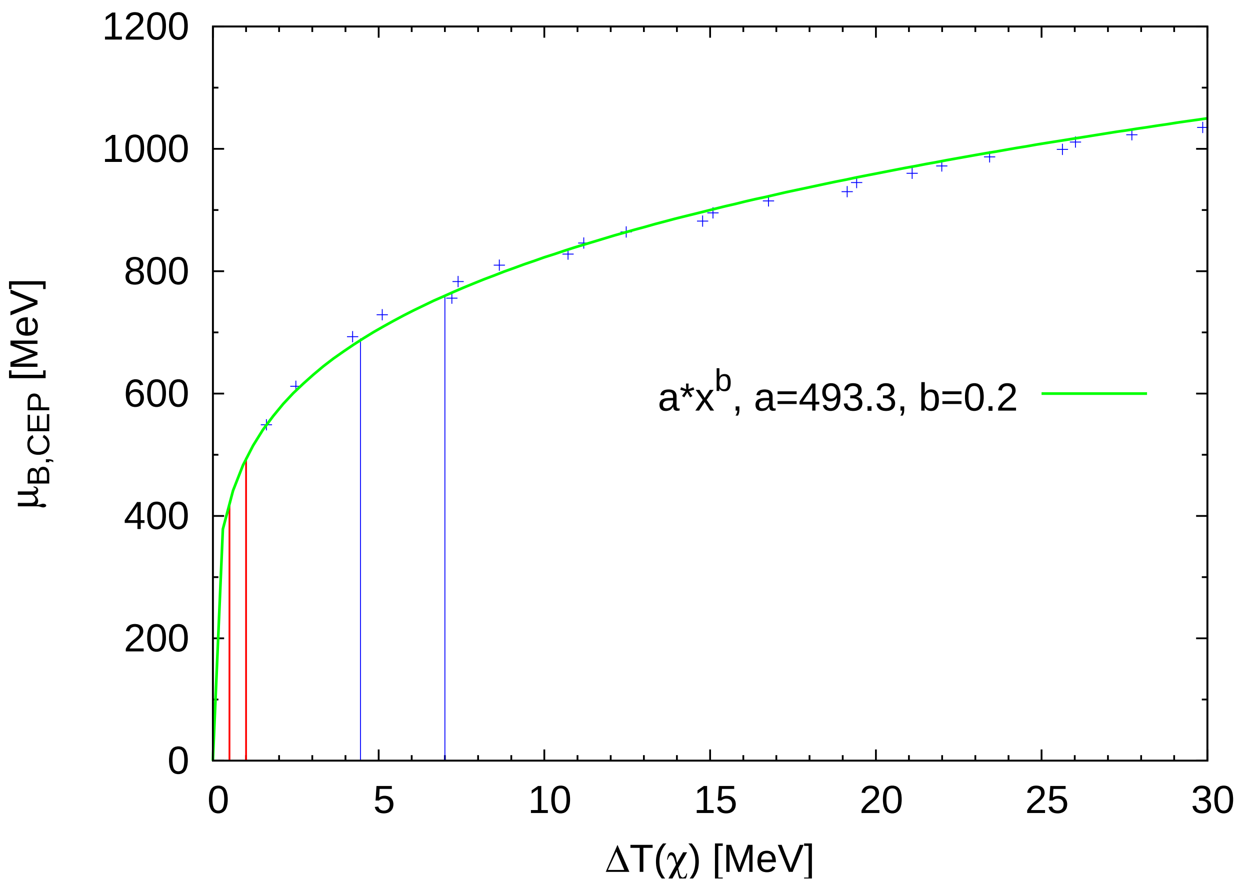

Preliminary lattice estimation by S. Katz: $\Delta T_c(\chi_{\bar{\psi}\psi}) \approx 0.5 - 1$ MeV
$\Delta T_c(\chi_{\bar{\psi}\psi}) \approx 2 - 4$ MeV

Since $\Delta T_c(\chi_{\bar{\psi}\psi}) \approx 28$ MeV at the physical point $\longrightarrow$ higher $\mu_{B,CEP}$ expected

The critical region of the CEP

Elongation of the critical region

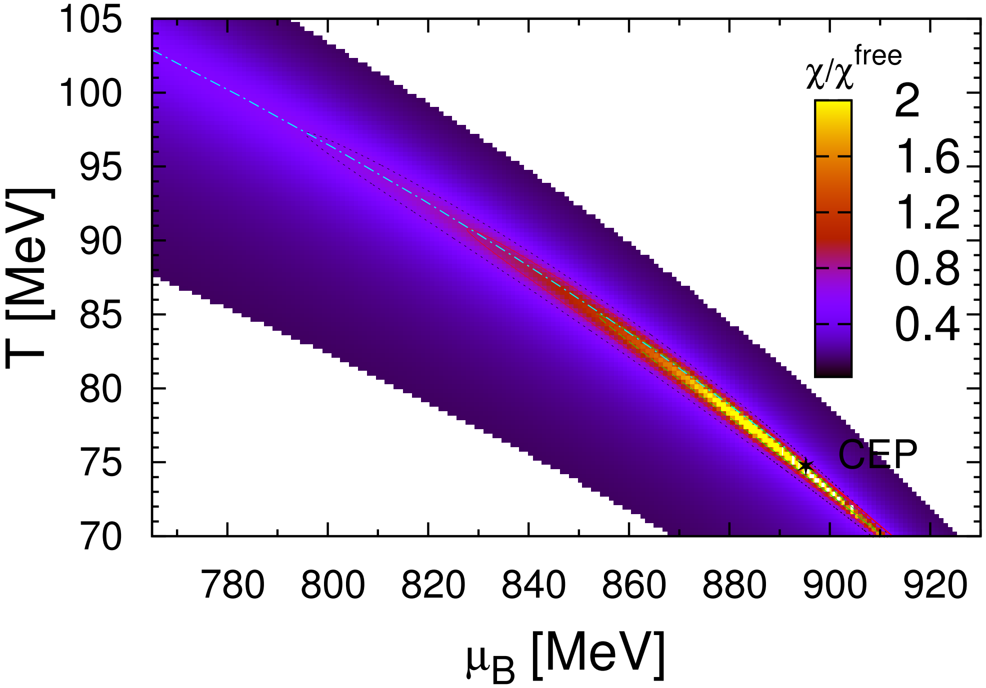

Scaling for asymptotically parallel path

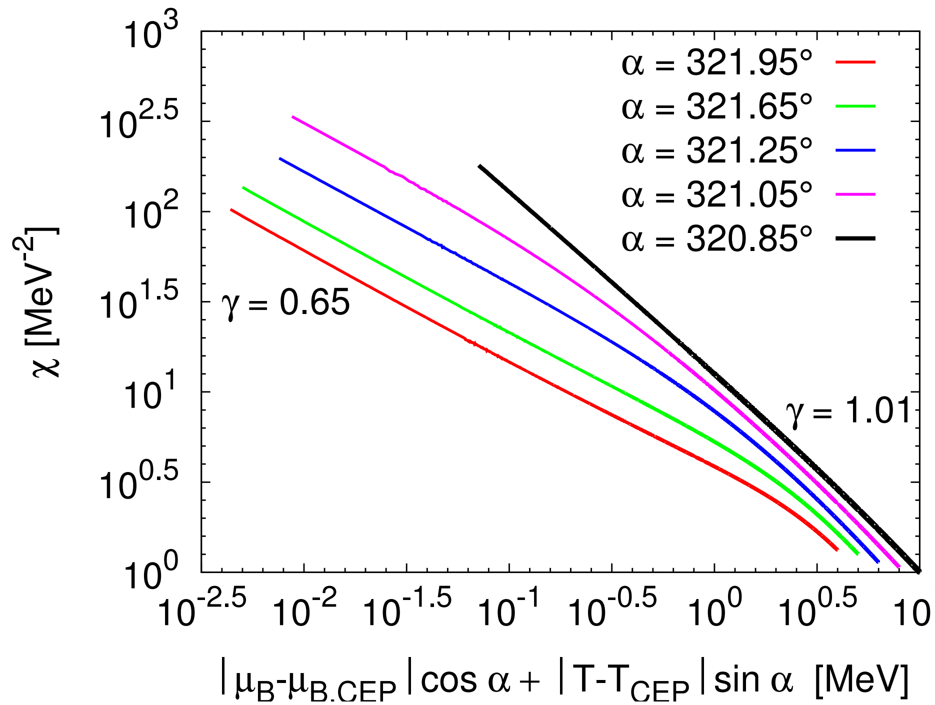

For the asymptotically parallel path we get $\gamma = 1.01$, which corresponds to the mean-field Ising exponent.

$\longrightarrow$ This path is the tangent line of the phase boundary curve at the CEP in the $\mu_B - T$ plane.

Introduction of chemical potentials

21 particles:

	pseudoscalars	$\pi^0, \eta, \eta', \pi^+, \pi^-, K^+, K^-, K^0, \bar{K}^0$
	scalars	$\sigma, a_0^0, f_0, a_0^+, a_0^-, \kappa^+, \kappa^-, \kappa^0, \bar{\kappa}^0$
	fermions	m_u, m_d, m_s

Lagrangian is invariant under

$$
\begin{aligned}
M &\rightarrow e^{-i\alpha_G G} M e^{i\alpha_G G} = M - i\alpha_G [G, M] + \mathcal{O}(\alpha_G^2), \\
\psi &\rightarrow e^{-i\alpha_G G}\psi = \psi - i\alpha_G \psi + \mathcal{O}(\alpha_G^2),
\end{aligned}
$$

where G can be $B = \sqrt{\frac{3}{2}}\lambda_0$, $I = \frac{1}{2}\lambda_3$ and $Y = \frac{1}{\sqrt{3}}\lambda_8$

The conserved Noether currents:

$$
J_\mu^G = -\frac{\delta L}{\delta(\partial^\mu M)_{ij}} i[G, M]_{j,i} - \frac{\delta L}{\delta(\partial^\mu M^+)_{ij}} i[G, M^+]_{j,i} - \frac{\delta L}{\delta(\partial^\mu \psi_i)} iG_{ij}\psi_j
$$

The conserved charges:

$$Q^B = \frac{1}{3}(N_u + N_d + N_s - N_{\bar{u}} - N_{\bar{d}} - N_{\bar{s}}),$$

$$Q^I = \frac{1}{2}(N_u - N_{\bar{u}} - N_d + N_{\bar{d}} + N_{\kappa^+} - N_{\kappa^-} + N_{\bar{\kappa}^0} - N_{\kappa^0} + N_{K^+} - N_{K^-} + N_{\bar{K}^0} - N_{K^0})$$
$$+ \quad N_{a_0^+} - N_{a_0^-} + N_{\pi^+} - N_{\pi^-},$$

$$Q^Y = \frac{1}{3}(N_u - N_{\bar{u}} + N_d - N_{\bar{d}} - 2N_s + 2N_{\bar{s}}) + N_{\kappa^+} - N_{\kappa^-} + N_{\kappa^0} - N_{\bar{\kappa}^0} + N_{K^+} - N_{K^-} + N_{K^0} - N_{\bar{K}^0}$$

Statistical density matrix of the system:

$$\rho = \exp[-\beta(H - \mu_i N_i)]$$

The following chemical potencials can be introduced:

$$\begin{aligned}
\mu_u &= -\mu_{\bar{u}} = \frac{1}{3}\mu_B + \frac{1}{2}\mu_I + \frac{1}{3}\mu_Y, \\
\mu_d &= -\mu_{\bar{d}} = \frac{1}{3}\mu_B - \frac{1}{2}\mu_I + \frac{1}{3}\mu_Y, \\
\mu_s &= -\mu_{\bar{s}} = \frac{1}{3}\mu_B - \frac{2}{3}\mu_Y, \\
\mu_{a_0^+} &= \mu_{\pi^+} = -\mu_{a_0^-} = -\mu_{\pi^-} = \mu_I, \\
\mu_{\kappa^+} &= \mu_{K^+} = -\mu_{\kappa^-} = -\mu_{K^-} = \frac{1}{2}\mu_I + \mu_Y, \\
\mu_{\kappa^0} &= \mu_{K^0} = -\mu_{\bar{\kappa}^0} = -\mu_{\bar{K}^0} = -\frac{1}{2}\mu_I + \mu_Y
\end{aligned}$$

Finite temperature propagators of charged fields

For example the K^-, K^+ field operators:

$$K^-(x) = \int \frac{d^3\mathbf{p}}{(2\pi)^3}\frac{1}{\sqrt{2E_\mathbf{p}}}\left(a^+(\mathbf{p})e^{ip\cdot x} + b(\mathbf{p})e^{-ip\cdot x}\right)\Big|_{p_0=E_\mathbf{p}},$$

$$K^+(x) = \int \frac{d^3\mathbf{p}}{(2\pi)^3}\frac{1}{\sqrt{2E_\mathbf{p}}}\left(b^+(\mathbf{p})e^{ip\cdot x} + a(\mathbf{p})e^{-ip\cdot x}\right)\Big|_{p_0=E_\mathbf{p}}$$

The two-point functions:

$$G_{K^-}(y-x) := \langle TK^-(y)K^+(x)\rangle_\beta = \Theta(y_0-x_0)\langle K^-(y)K^+(x)\rangle_\beta + \Theta(x_0-y_0)\langle K^+(x)K^-(y)\rangle_\beta,$$

$$G_{K^+}(y-x) := \langle TK^+(y)K^-(x)\rangle_\beta = \Theta(y_0-x_0)\langle K^+(y)K^-(x)\rangle_\beta + \Theta(x_0-y_0)\langle K^-(x)K^+(y)\rangle_\beta,$$

In momentum space the finite temperature propagators:

$$G_{K^-}(k) = \frac{i}{2E_\mathbf{k}}\left[\frac{1+n_{K^-}(E_\mathbf{k})}{k_0-E_\mathbf{k}+i\epsilon} - \frac{n_{K^-}(E_\mathbf{k})}{k_0-E_\mathbf{k}-i\epsilon} - \frac{1+n_{K^+}(E_\mathbf{k})}{k_0+E_\mathbf{k}-i\epsilon} + \frac{n_{K^+}(E_\mathbf{k})}{k_0+E_\mathbf{k}+i\epsilon}\right]$$

$$G_{K^+}(k) = \frac{i}{2E_\mathbf{k}}\left[\frac{1+n_{K^+}(E_\mathbf{k})}{k_0-E_\mathbf{k}+i\epsilon} - \frac{n_{K^+}(E_\mathbf{k})}{k_0-E_\mathbf{k}-i\epsilon} - \frac{1+n_{K^-}(E_\mathbf{k})}{k_0+E_\mathbf{k}-i\epsilon} + \frac{n_{K^-}(E_\mathbf{k})}{k_0+E_\mathbf{k}+i\epsilon}\right]$$

Self-energies

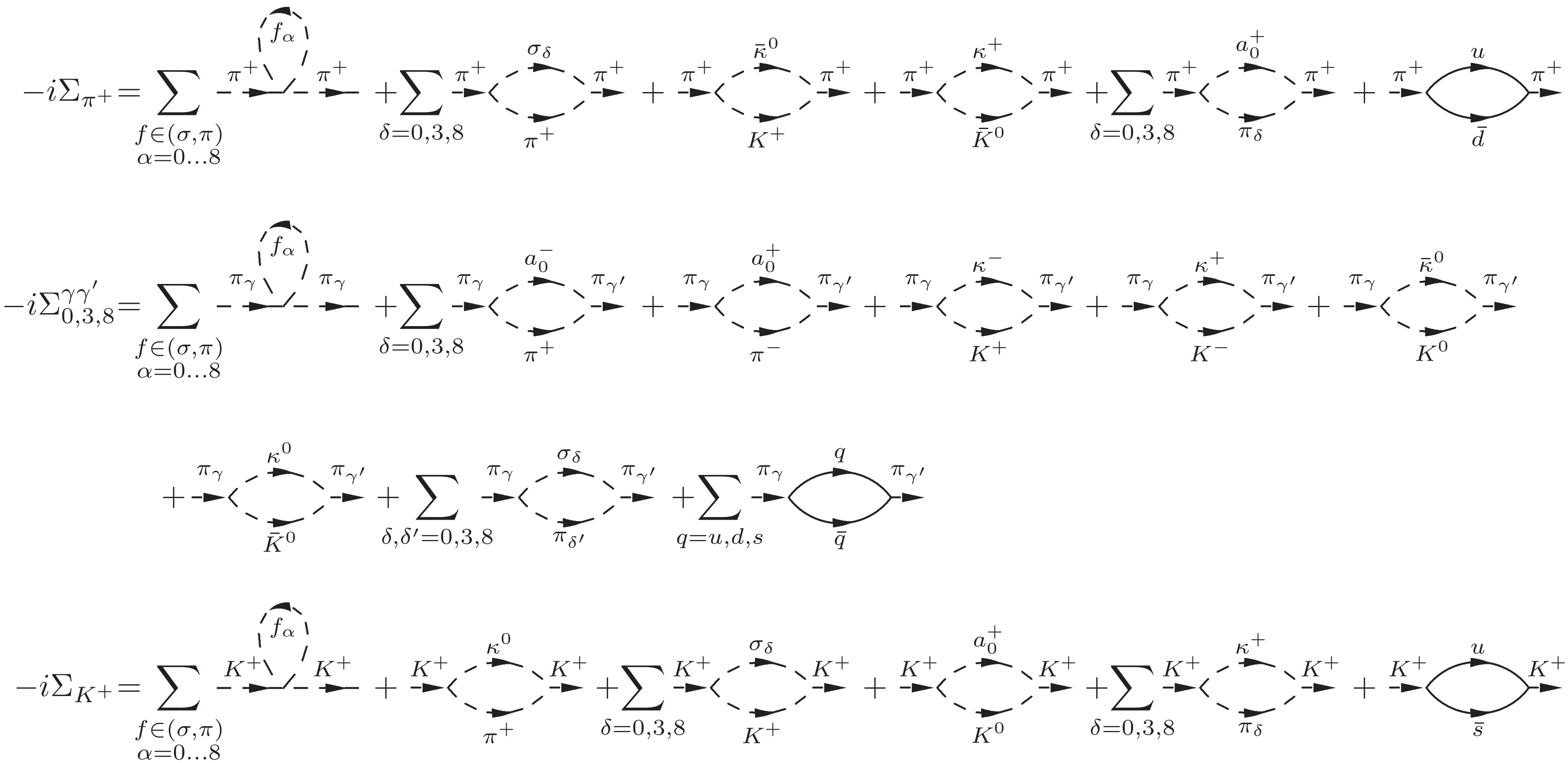

Temperature dependence of v_3

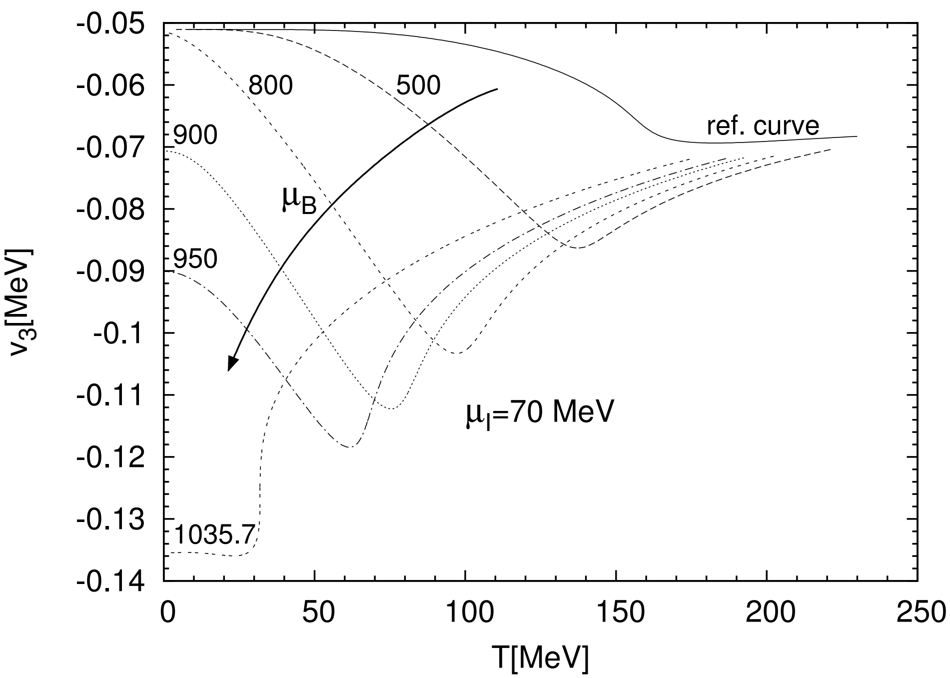

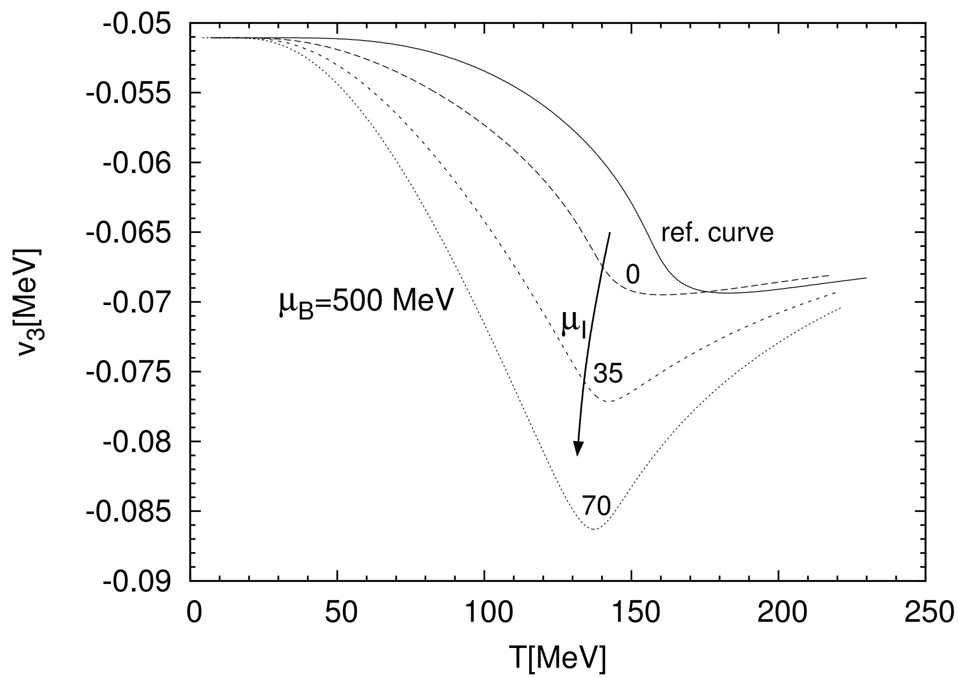

On the left Fig.: μ_B dpendence at a given μ_I

Lowest curve correspond to a CEP

v_3 at $T = 0$ significantly depend on μ_B

On the left Fig.: μ_I dpendence at a given μ_B

Increasing of either μ_B or μ_I $\longrightarrow$ influence of v_3 becomes stronger

CEP at $\mu_I = 0$: $T_{\rm CEP} = 63.08$ MeV, $\mu_{B,\rm CEP} = 960.8$ MeV$\rightarrow$ large diff. to case $v_3 = 0$

Reason: x and v_3 related $\longrightarrow$ common transition point

Dependence of the CEP on μ_I, μ_Y

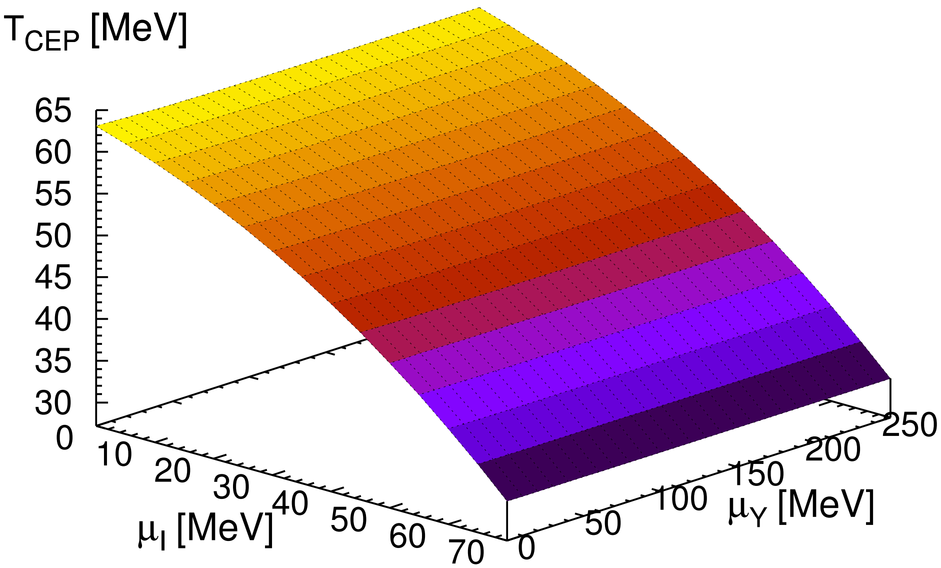

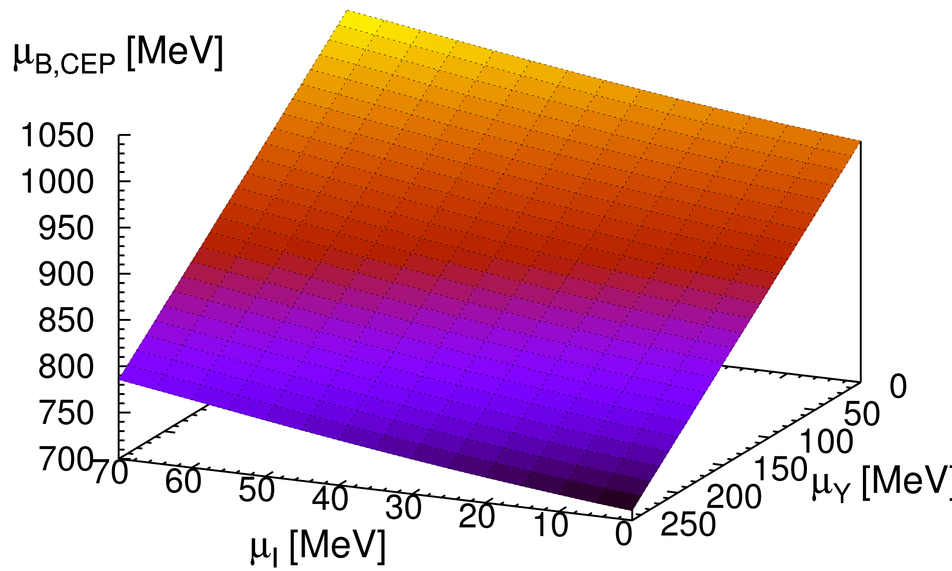

T_{CEP} is almost independent of μ_Y, but significantly depend on μ_I

$\mu_{B,\mathrm{CEP}}$ has an almost linear dependence on both other chenical potential

As μ_Y is increased the phase transition at $T = 0$ becomes stronger

Conclusions and outlook

- The best parametrization of the model gives first order / crossover type phase transition at $T = 0$ / $\mu_B = 0$ as a function of μ_B / T of the physical point.
- The 2^{nd} order surface was determined in the $m_\pi - m_K - \mu_B$ space using ChPT to obtain the m_π,m_K dependence of the couplings and of the constituent quark masses.
- The CEP was located at the physical point:
  $T_{CEP} = 74.83$ MeV $\mu_{B,CEP} = 895.38$ MeV.
- The dependence of the μ_B on the width of the susceptibility was investigated.
- The scaling properities were studied and the Ising temperature direction was found at the CEP.
- Effects of isospin and hyper chemical potential on the CEP was investigated.
  $T_{CEP} = 63.08$ MeV $\mu_{B,CEP} = 960.8$ MeV at $\mu_I = 0$ ($v_3 \neq 0$ at $T = 0$).
- In progress: μ_I dependence of different pole masses and the study of pion condensation.